

**Aluminum Incorporated *p*-CuO/*n*-ZnO Photocathode Coated with Nanocrystal  
Engineered TiO<sub>2</sub> Protective Layer for Photoelectrochemical Water Splitting and  
Hydrogen Generation**

Saeid Masudy-Panah,<sup>1,2</sup> Eugene Y.-J. Kong,<sup>1</sup> Negar Dasineh Khiavi,<sup>3</sup> Reza Katal,<sup>4</sup> and Xiao  
Gong<sup>1,2</sup>

<sup>1</sup>Electrical and Computer Engineering, National University of Singapore, Singapore 119260

<sup>2</sup>Low Energy Electronic Systems (LEES), Singapore-MIT Alliance for Research and  
Technology (SMART) Centre, Singapore

<sup>3</sup>Faculty of Biosciences & Medical Engineering, Universiti Teknologi Malaysia

<sup>4</sup>Department of Civil & Environmental Engineering, National University of Singapore,  
Singapore 119260

Corresponding author e-mail: [elegong@nus.edu.sg](mailto:elegong@nus.edu.sg)

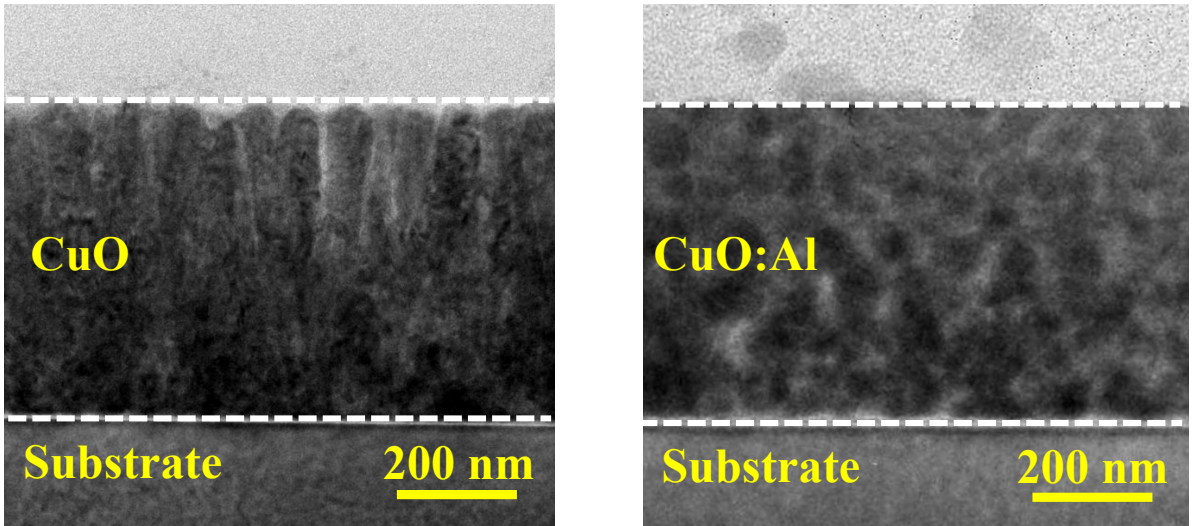


**Figure S1.** Cross-sectional TEM images of (a) CuO and (b) CuO:Al thin films deposited at CuO sputtering power of 300 W and Al sputtering power of 12 W. The thickness of the CuO and CuO:Al is ~500 nm.

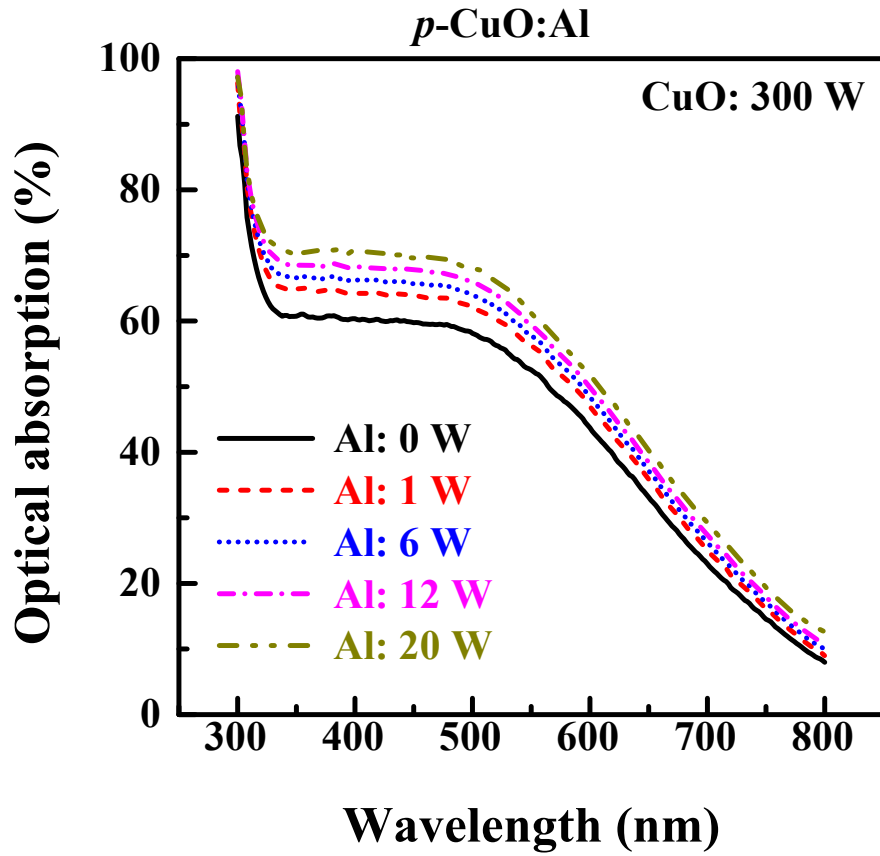


**Figure S2.** Absorption spectra of *p*-CuO:Al thin films deposited with Al sputtering power of 0-20 W. Optical absorption is enhanced with increasing Al incorporation.

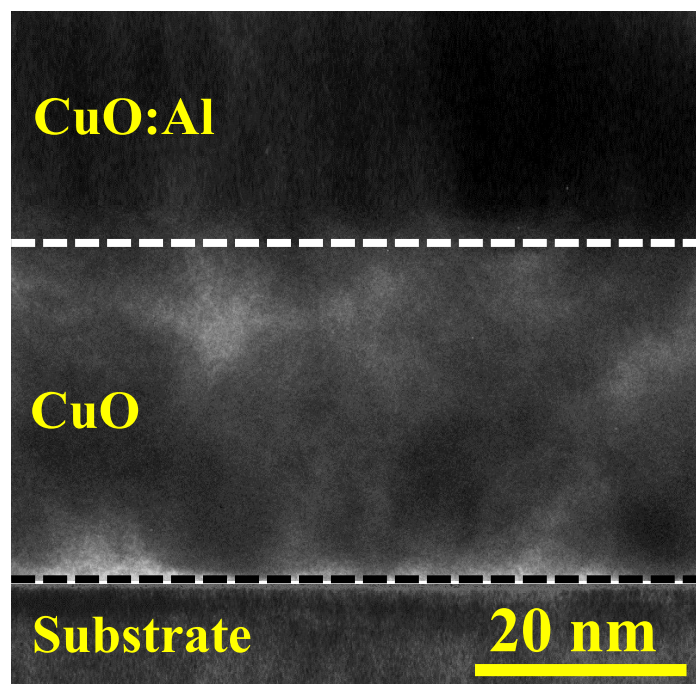


**Figure S3.** Cross-sectional TEM image of the 30-nm-thick CuO interfacial layer inserted below the CuO:Al film in a *p*-(CuO/CuO:Al) photocathode.

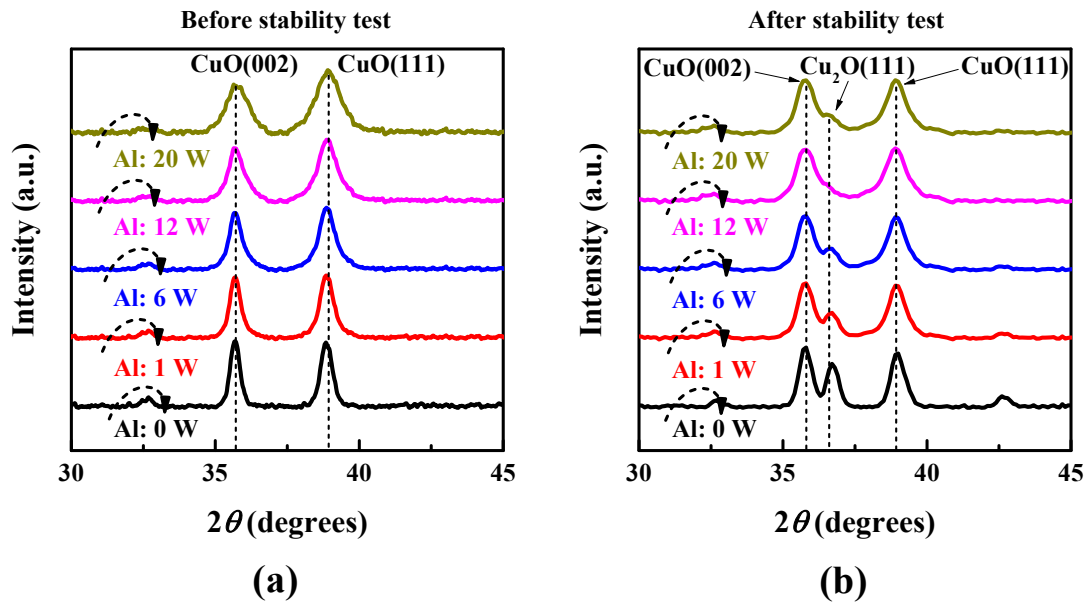


**Figure S4.** XRD spectra of *p*-(CuO/CuO:Al) photocathodes (a) before and (b) after photocorrosion stability test. An additional Cu<sub>2</sub>O(111) XRD peak at  $2\theta$  of 36.45 degrees can be found for both CuO and CuO:Al photocathodes after photocorrosion stability test, but the intensity of this peak is weaker in the CuO:Al photocathodes.

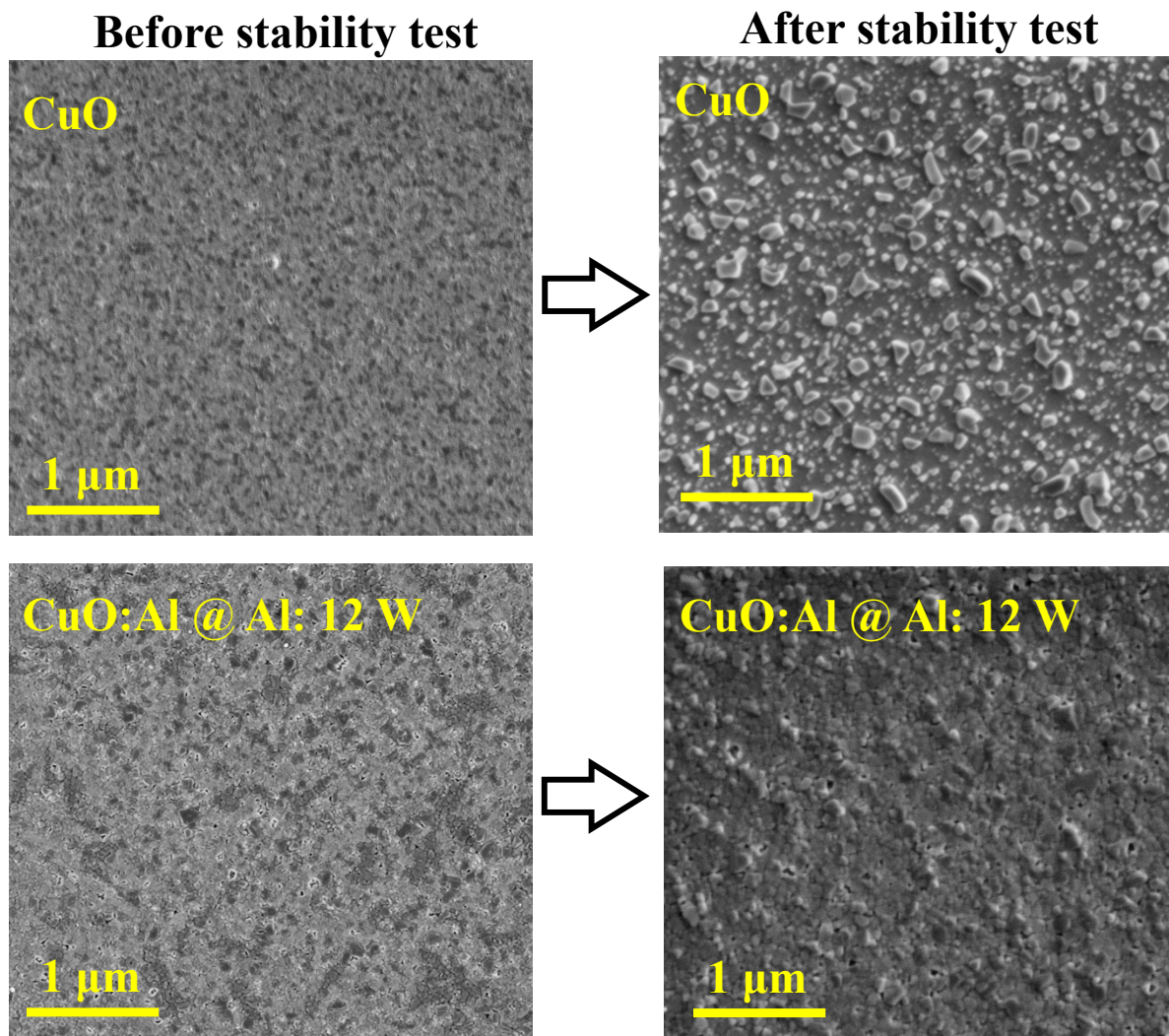


**Figure S5.** Top-view SEM images of the CuO and CuO:Al (@ Al: 12 W) photocathodes (a) before and (b) after photocorrosion stability test. Formation of small islands after the photocorrosion stability test, which is mainly caused by the reduction of CuO to Cu<sub>2</sub>O, is reduced for the CuO:Al photocathode.

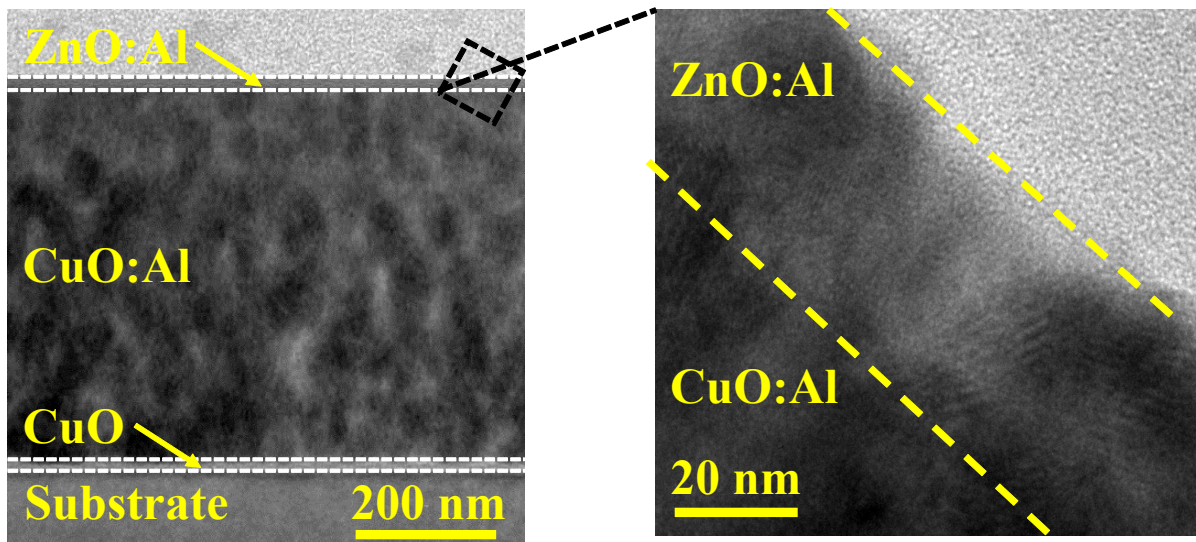
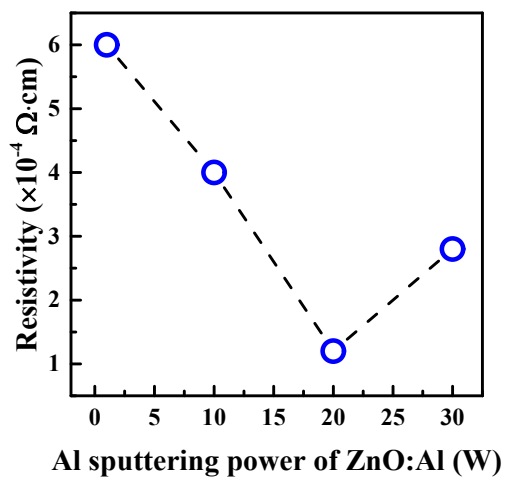
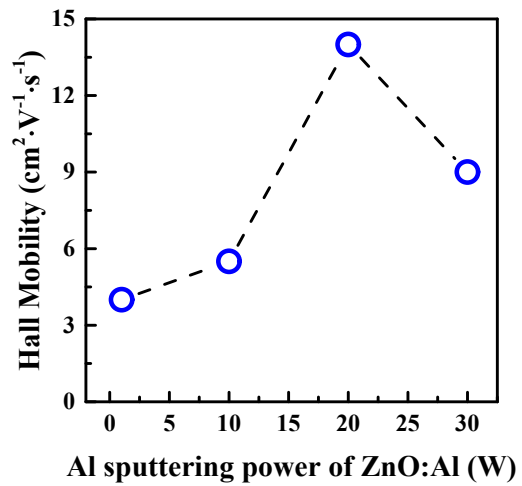


**Figure S6.** (a) Cross-sectional and (b) high-resolution TEM images of a  $p$ -(CuO/CuO:Al)/ $n$ -ZnO:Al photocathode fabricated with Al sputtering power of 20 W during ZnO:Al deposition. The thickness of the ZnO:Al layer is  $\sim 20$  nm.





(a)



(b)

**Figure S7.** (a) Electrical resistivity and (b) hall mobility of thin sputter-deposited ZnO:Al films on glass substrate. The Al concentration in ZnO significantly influences its electrical resistivity and hall mobility.



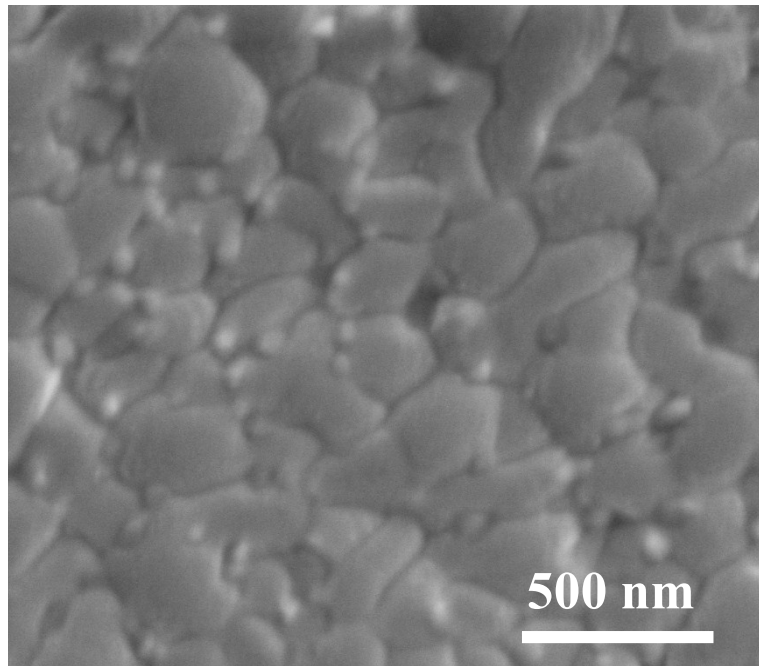
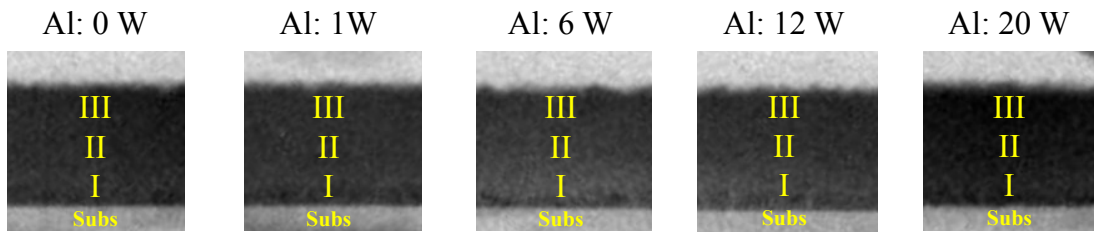


**Figure S8.** Top-view SEM image of a  $p$ -(CuO/CuO:Al)/ $n$ -ZnO:Al/TiO<sub>2</sub>/Au-Pd photocathode. The Au-Pd nanoparticles are randomly and uniformly distributed on the TiO<sub>2</sub> protective layer.

Table SI. Results of energy-dispersive X-ray spectroscopy (EDS) analysis of the CuO:Al thin films prepared at CuO sputtering power of 300 W and different Al sputtering power.



| Region | Al: 0 W |     |    | Al: 1 W |       |      | Al: 6 W |       |    | Al: 12 W |       |    | Al: 20 W |       |    |
|--------|---------|-----|----|---------|-------|------|---------|-------|----|----------|-------|----|----------|-------|----|
|        | Cu      | O   | Al | Cu      | O     | Al   | Cu      | O     | Al | Cu       | O     | Al | Cu       | O     | Al |
| I      | 51%     | 49% | 0% | 50.2%   | 49.3% | 0.5% | 49.5%   | 48.5% | 2% | 48.5%    | 47.5% | 4% | 47.5%    | 46.5% | 6% |
| II     | 51%     | 49% | 0% | 50%     | 49.5% | 0.5% | 49%     | 49%   | 2% | 48%      | 48%   | 4% | 47%      | 47%   | 6% |
| III    | 50%     | 50% | 0% | 50%     | 49.5% | 0.5% | 49%     | 49%   | 2% | 48%      | 48%   | 4% | 47%      | 47%   | 6% |

Table SII. Cu, O, and Al percentages in the CuO:Al (Al: 0, 1, 6, 12, and 20 W) samples, calculated from XPS analysis.

|        | <b>Al: 0 W</b> | <b>Al: 1 W</b> | <b>Al: 6 W</b> | <b>Al: 12 W</b> | <b>Al: 20 W</b> |
|--------|----------------|----------------|----------------|-----------------|-----------------|
| Cu (%) | 50             | 49.4           | 49.1           | 48.15           | 46.9            |
| O (%)  | 50             | 49.2           | 49             | 48.1            | 46.8            |
| Al (%) | 0              | 0.4            | 1.9            | 3.75            | 6.3             |